

Preparation of peptide-conjugated quantum dots for tumor vasculature-targeted imaging

Weibo Cai & Xiaoyuan Chen

Molecular Imaging Program at Stanford (MIPS), Department of Radiology and Bio-X Program, Stanford University School of Medicine, Stanford, California 94305, USA. Correspondence should be addressed to X.C. (shawchen@stanford.edu).

Published online 10 January 2008; doi:10.1038/nprot.2007.478

To take full advantage of the unique optical properties of quantum dots (QDs) and expedite future near-infrared fluorescence (NIRF) imaging applications, QDs need to be effectively, specifically and reliably directed to a specific organ or disease site after systemic administration. Recently, we reported the use of peptide-conjugated QDs for non-invasive NIRF imaging of tumor vasculature markers in small animal models. In this protocol, we describe the detailed procedure for the preparation of such peptide-conjugated QDs using commercially available PEG-coated QDs and arginine-glycine-aspartic acid (RGD) peptides. Conjugation of the thiolated RGD peptide to the QDs was achieved through a heterobifunctional linker, 4-maleimidobutyric acid *N*-succinimidyl ester. Competitive cell binding assay, using ¹²⁵I-echistatin as the radioligand, and live cell staining were carried out to confirm the successful attachment of the RGD peptides to the QD surface before *in vivo* imaging of tumor-bearing mice. In general, QD conjugation and *in vitro* validation of the peptide-conjugated QDs can be accomplished within 1–2 d; *in vivo* imaging will take another 1–2 d depending on the experimental design.

INTRODUCTION

QDs are fluorescent semiconductor nanoparticles with many unique optical properties suitable for multiplexed *in vitro* and *in vivo* imaging^{1–3}. Numerous *in vitro* and cell-based applications have been discovered for QDs^{4,5}. In the near-infrared (700–900 nm) region, the absorbance spectra for most biomolecules reach minimum, which provides a clear window for *in vivo* optical imaging⁶. A vast number of literature is available where nontargeted QDs were used for cell trafficking^{7,8}, vasculature imaging^{9,10}, sentinel lymph node mapping^{11,12} and neural imaging¹³. To make QDs more useful for *in vivo* imaging and other biomedical applications, QDs need to be effectively, specifically and reliably directed to a specific organ or disease site without alteration. Specific targeting can be achieved by attaching targeting molecules to the QD surface. Peptides, peptidomimetics and small molecules are suitable targeting ligands, as large numbers of these molecules can be linked to the surface of a single QD and such conjugates may exhibit strong receptor binding affinity and desirable targeting efficacy due to the polyvalency effect¹⁴.

Angiogenesis, the formation of new blood vessels from the preexisting vasculature, is essential for tumor growth and progression^{15–17}. Integrin $\alpha_v\beta_3$, a cell adhesion molecule, is significantly upregulated in invasive tumor cells of many cancer types and most tumor vasculature but not in quiescent endothelium and normal tissues^{18,19}. The fact that integrin $\alpha_v\beta_3$ is overexpressed on both tumor vasculature and tumor cells makes it a prime target for *in vivo* targeted imaging using QD-based probes, as extravasation is not required to observe tumor signal. We recently reported the *in vivo* targeted imaging of tumor vasculature using peptide-conjugated QDs²⁰. In this study, RGD (potent integrin $\alpha_v\beta_3$ antagonist)-containing peptides were conjugated to QD705 (emission maximum at 705 nm) and QD705-RGD exhibited high-affinity integrin $\alpha_v\beta_3$ specific binding in cell culture, *ex vivo*, and in living mice bearing subcutaneous integrin $\alpha_v\beta_3$ -positive U87MG human glioblastoma tumors.

The protocol described here provides a step-by-step procedure for the preparation of this QD705-RGD conjugate and its subsequent

use for cell staining and *in vivo* targeted imaging. The chemistry of preparing this conjugate can be employed to attach other thiol-containing ligands to any amino functionalized QDs (Fig. 1). The QD705 used in this study contains a polyethylene glycol (PEG; MW 2 kDa) spacer covalently attached to the QD surface, resulting in improved stability in high-salt buffers and reduced nonspecific binding. We found that carboxyl-modified QDs that do not contain PEG spacers may precipitate from high-salt buffers. Moreover, the significantly more nonspecific binding to cells compared to the amino functionalized QDs also makes the experimental findings harder to interpret. As both QD705 and the RGD peptide contain amino groups, conjugation through a heterobifunctional linker (e.g., 4-maleimidobutyric acid *N*-succinimidyl ester) after converting one of the amino group to a thiol group is the most convenient and widely used approach²¹. Alternatively, reacting excess amount of a homobifunctional linker (e.g., one with two *N*-succinimidyl esters) with either QD705 or the RGD peptide, which, upon purification, is conjugated to the other agent, may also be employed. However, this approach was not widely used in the literature, and it is also difficult to control the reaction in certain cases.

The major limitation of this protocol does not lie in the chemistry itself but in choosing the appropriate target. QD705, as well as QD705-RGD, has rather short circulation half-life and very rapid uptake in the reticuloendothelial system. Thus, there is not enough circulation time to allow for efficient extravasation of QD705-RGD to target the tumor cells. The expression level of integrin $\alpha_v\beta_3$ is very high on the U87MG tumor vasculature^{22,23}. Therefore, even with almost exclusive tumor vasculature targeting, we were able to observe good tumor-to-background contrast. With future development of small, biocompatible, long-circulating QDs, it may become possible to target both the tumor vasculature and the tumor cells.

For *in vitro* testing of QD705-RGD, cells with high and low integrin $\alpha_v\beta_3$ expression, for example, U87MG human glioblastoma and MCF-7 human breast cancer cells^{22,24}, can serve as positive and negative controls. For *in vivo* imaging, tumors with low

PROTOCOL

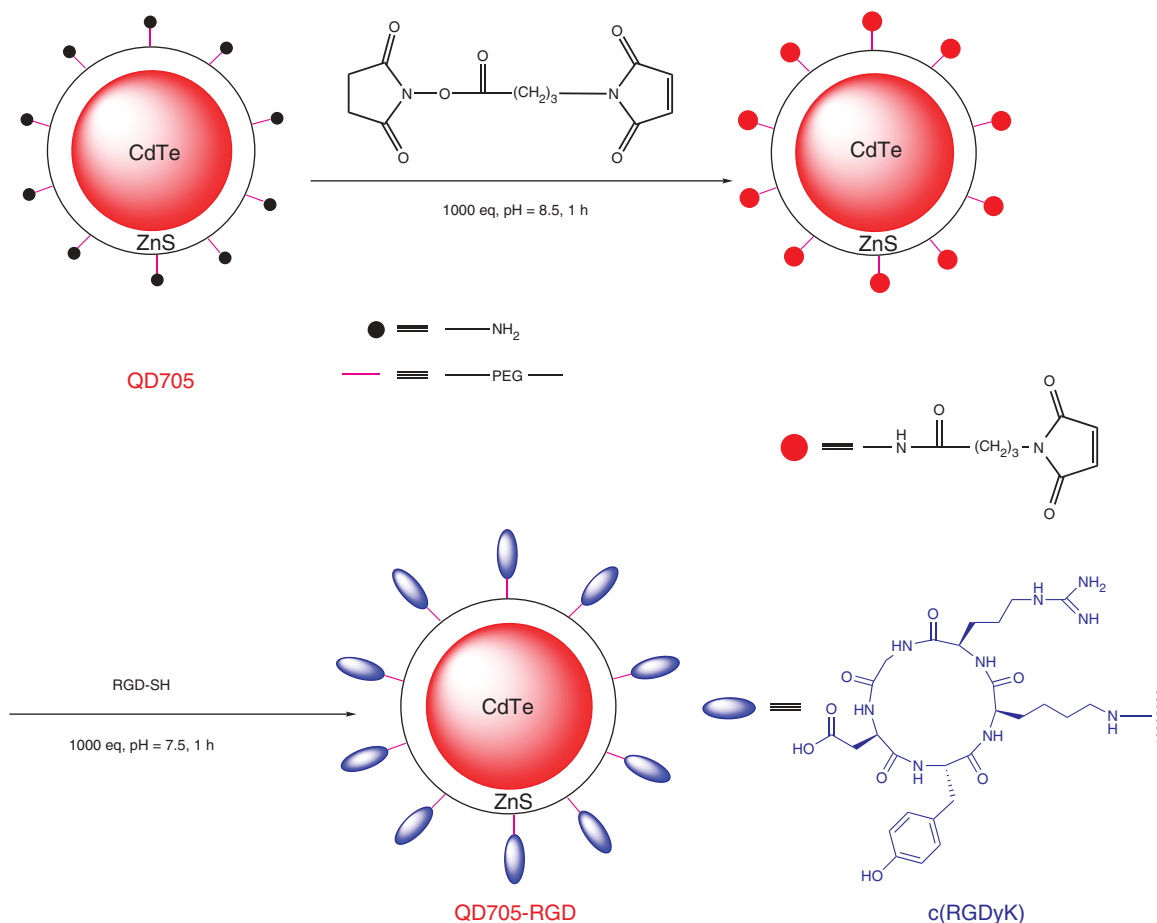


Figure 1 | Synthesis of QD705-RGD. equiv., equivalent; PEG, polyethylene glycol (MW 2 kDa).

integrin $\alpha_v\beta_3$ expression, as well as QD705 without RGD conjugation, can serve as valid negative controls. Both *in vitro* and *in vivo* receptor blocking experiments with unconjugated RGD peptide can also be performed to further confirm the integrin $\alpha_v\beta_3$ specificity of QD705-RGD. To obtain statistically meaningful results, at least three samples or animals per group are needed.

QD-based NIRF imaging in small animals cannot be directly scaled up to *in vivo* imaging in patients due to the limited optical signal penetration depth. In clinical settings, fluorescence imaging

is relevant for tissues close to the surface of the skin and tissues accessible by endoscopy and intraoperative visualization. The major roadblocks for clinical translation of QD-based agents are inefficient delivery, potential toxicity and lack of quantification¹. However, with the development of smaller^{12,25}, less-toxic²⁶, self-illuminating^{27,28}, multifunctional QDs^{29,30} and further improvement of the conjugation strategy, it is expected that QD-based probes may achieve optimal tumor-targeting efficacy with acceptable toxicity profile for clinical translation in the near future.

MATERIALS

REAGENTS

- QDs (Qdot 705 ITK amino (PEG) QDs; Invitrogen, cat. no. Q21561MP)
- 4-Maleimidobutyric acid *N*-succinimidyl ester (Sigma, cat. no. M7642)
- 10 mM sodium borate buffer, pH 8.5 (Sigma, cat. no. 71997)
- PBS buffer (Invitrogen, cat. no. 20012-027)
- RGD peptide (c(RGDyK); Peptides International)
- *N*-Succinimidyl *S*-acetylthioacetate (Pierce Biotechnology Inc., cat. no. 26102)
- DMSO (ACROS, cat. no. 61097-1000)
- High-performance liquid chromatography (HPLC)-grade acetonitrile (Fisher Scientific, cat. no. A998-4)
- Trifluoroacetic acid (Fisher Scientific, cat. no. AC139721000)
- Hydroxylamine hydrochloride (Sigma, cat. no. 255580)
- Tris(2-carboxyethyl)phosphine hydrochloride (TCEP.HCl; Pierce Biotechnology Inc., cat. no. 20490)

- Sodium hydroxide (Sigma, cat. no. 367176)
- Hydrochloric acid (Sigma, cat. no. H3162)
- Thiolated RGD peptide (see **Box 1** and **Fig. 2**)
- U87MG human glioblastoma cells (ATCC, cat. no. HTB-14; see REAGENT SETUP)
- MCF-7 human breast cancer cells (ATCC, cat. no. HTB-22; see REAGENT SETUP)
- Low-glucose DMEM (GIBCO, cat. no. 11885-084)
- Minimum essential medium (GIBCO, cat. no. 11095-080)
- Fetal bovine serum (FBS; GIBCO, cat. no. 10437-028)
- Cell-binding buffer (20 mM Tris, 150 mM NaCl, 2 mM CaCl₂, 1 mM MnCl₂, 1 mM MgCl₂, 0.1% (wt/vol) bovine serum albumin; pH 7.4)
- ¹²⁵I-Echistatin (GE Healthcare, cat. no. IM304) **! CAUTION** It is imperative to obtain appropriate training from the institutional radiation safety office before receiving radioactivity. Abide by all relevant regulatory rules and use

BOX 1 | PREPARATION OF THIOLATED RGD PEPTIDE

The procedure described here was based on our previous report (Fig. 2) (see ref. 37). Alternative methods to synthesize thiolated RGD peptide (RGD-SH) include the use of Traut's agent³⁸ or other heterofunctional agents (where one end reacts with the amino group and the other end contains a protected sulfhydryl group that can be readily deprotected).

1. Mix c(RGDyK) (5 μmol) in 1 ml of borate buffer (pH 8.5) with 100 μl of DMSO solution containing 6 μmol of SATA.
2. Monitor the reaction by analytical RP-HPLC (reverse phase-high performance liquid chromatography). In a typical setup, the mobile phase is changed from 95% solvent A (0.1% TFA in water) and 5% solvent B (0.1% TFA in acetonitrile) (0–2 min) to 35% solvent A and 65% solvent B at 32 min. The flow rate was 1 ml min^{-1} and the UV absorbance was monitored at 218 nm. The HPLC retention time (R_t) for c(RGDyK) and SATA-c(RGDyK) were 7.9 and 12.1 min, respectively.
3. When the reaction has gone to completion, quench with 100 μl of 2% TFA in water.
4. Freeze-dry the crude mixture and redissolve it in 1 ml of water.
5. Add 100 μl of 0.5 M hydroxylamine solution. Adjust the pH to 6.0 (pipette 1–5 μl of the reaction mixture and apply it to a pH paper) with 0.5 M sodium hydroxide or hydrochloric acid solution if needed.

▲ CRITICAL STEP If the pH of the reaction mixture is too low, it may result in incomplete de-protection of the thiol. If the pH of the reaction mixture is too high, disulfide bond may form when the thiol group is released.

6. When the reaction has gone to completion based on analytical RP-HPLC, purify the RGD-SH by semi-preparative RP-HPLC. The gradient is the same as described above, but a semi-preparative HPLC column and a flow rate of 5 ml min^{-1} is used. The R_t for RGD-SH is 10.7 min ($C_{29}H_{43}N_9O_9S$, calculated 693.3, observed 694.5 ($[M + H]^+$). Collect the fractions containing pure RGD-SH and freeze-dry.
7. Store RGD-SH under acidic condition (pH 3–4) in water to prevent disulfide formation.

■ PAUSE POINT RGD-SH can be stored for up to a few months under acidic condition.

● TIMING

Steps 1–4 take about 1 d. Steps 5 and 6 are typically carried out on the following day. Step 6 may take a few hours up to a few days depending on the amount of crude RGD-SH to purify and how much crude mixture can be loaded onto the HPLC column per injection.

appropriate protection when handling radioactivity. Dispose of the ¹²⁵I-containing radioactive waste according to the institutional radioactive waste disposal guidelines.

- Isoflurane (RxElite Inc., cat. no. NDC60307-120-25)
- U87MG tumor-bearing athymic nude mice (Harlan; see REAGENT SETUP)
- ! **CAUTION** Please obtain appropriate training from the institution regarding animal handling. Animal protocols must be in place before performing animal studies.

EQUIPMENT

- HPLC (Dionex)
- Analytical HPLC column (Vydac, cat. no. 218TP25)
- Semi-preparative HPLC column (Vydac, cat. no. 218TP510)
- Freeze-dry system (Labconco Corp.)
- pH paper (EMD Chemicals Inc., cat. no. 9588-3 & 9586-3)
- NAP-10 column (GE Healthcare, cat. no. 17-0854-01)
- Refrigerated microcentrifuge (Eppendorf, 5417R)
- Fluorometer (FluoroMax-3; Jobin Yvon)
- 96-well plate (Thermolab Systems, cat. no. 7417)
- Vacuum manifold (Millipore, cat. no. MAVM0960R)
- Vacuum pump (VWR, cat. no. 89004-272)
- Dry bath incubator (Fisher Scientific, cat. no. 11-718-2)
- Polystyrene culture test tube (Fisher Scientific, cat. no. 14-961-10)
- γ -counter (Packard)
- GraphPad Prism (GraphPad Software Inc.)
- Glass-bottomed microwell dish (30-mm Petri dish, 14-mm microwell; MatTek, cat. no. P35G-0-14-C)
- Inverted fluorescence microscope (Zeiss)
- Microscope filter set (excitation, 420/40 nm; emission, 705/40 nm; Chroma Technology)
- IVIS imaging system (Xenogen; see EQUIPMENT SETUP)
- Maestro imaging system (CRI Inc.; see EQUIPMENT SETUP)
- Rodent anesthesia system (Summit Anesthesia Solutions)

PROCEDURE

Conjugation of QDs

- 1| Mix the following two reagents: QD705 (1 nmol (125 μl)) and 4-maleimidobutyric acid *N*-succinimidyl ester (1 μmol in 200 μl of borate buffer). Pipette 1–5 μl of the reaction mixture and apply it to a pH paper to make sure that the pH is about 8.5.
- 2| Incubate the mixture in an Eppendorf tube at room temperature (20 °C) for 1 h with gentle shaking.

REAGENT SETUP

U87MG and MCF-7 cells Culture U87MG cells in DMEM (low glucose) supplemented with 10% (vol/vol) FBS at 37 °C. Culture MCF-7 cells in MEM supplemented with 10% (vol/vol) FBS at 37 °C. The cells should be used when they reach 70–85% confluency. For cell staining, 0.05–0.1 million cells per Petri dish are needed. For cell binding assay, 0.1 million cells per well are needed. Triplicate samples are recommended to obtain statistically meaningful results.

U87MG tumor model The animals can be used for *in vivo* imaging studies when the U87MG tumor size reaches about 500 mm^3 . Typically, we inject 5×10^6 U87MG cells subcutaneously into athymic nude mice, and it takes 3–4 weeks for the tumor to reach such a size^{31,32}. The tumor size can be calculated as $a \times b^2/2$ ('a' represents the longer dimension and 'b' represents the shorter dimension of the tumor). ! **CAUTION** Please obtain appropriate training from the institution regarding animal handling and have animal protocols in place before performing animal studies.

EQUIPMENT SETUP

The Maestro and the IVIS Systems Both systems are quite user friendly once the user has gone through appropriate training of the systems. The key issue is choosing the right excitation/emission filter sets for *in vivo* imaging. QDs can be excited at any wavelength shorter than their emission wavelength, and the shorter the excitation wavelength, the stronger the absorbance and fluorescence^{1,2}. However, tissue penetration at shorter wavelength is much poorer. We compared a limited set of excitation filters available in our imaging systems and found that the 590/30 nm excitation gave the best result and the shortest image acquisition time. Excitation at shorter wavelength such as 525/50 nm had dramatically lower fluorescence signal due to poor tissue penetration, although QD705-RGD has much stronger absorbance at this wavelength than at 590 nm. The filter sets we used to acquire the images shown in this protocol are described below. Maestro: excitation, 590/30 nm; emission, 645-nm-long pass. IVIS: excitation, 525/50 nm; emission, 730/80 nm.

PROTOCOL

3| Equilibrate an NAP-10 column with PBS.

4| Load the reaction mixture onto the NAP-10 column; wait until all the mixture is in the column. Add 2 ml of PBS and collect only the deepest-colored fractions (usually 200–400 μl). A hand-held UV lamp can help with the visualization.

5| Add 1 μmol of RGD-SH (thiolated RGD peptide) dissolved in minimum volume of PBS into the QD705 solution, and adjust the pH to 7.0–7.5 (based on pH paper) with borate buffer if necessary.

▲ CRITICAL STEP It is highly recommended to check the purity of the RGD-SH by analytical HPLC before conjugation. If significant amount of disulfide already formed, some TCEP.HCL (~ 1 mg or less) can be added to release the free thiol.

6| Incubate the mixture in an Eppendorf tube at room temperature for 1 h with gentle shaking.

7| Equilibrate another NAP-10 column with PBS.

8| Load the reaction mixture onto the NAP-10 column, wait until all the mixture is in the column, add 2 ml of PBS and collect only the deepest-colored fractions (usually 300–500 μl in total).

▲ CRITICAL STEP Collect multiple small fractions of the eluent (typically every two drops). Use the most concentrated fraction(s) for future *in vivo* imaging. Although such procedure may not completely remove all the unreacted RGD-SH, the residual unreacted RGD-SH should not significantly affect future experiments. The most concentrated QD705-RGD fractions should be in the 1–4 μM range, suitable for *in vivo* imaging.

9| Store the collected fractions at 4 $^{\circ}\text{C}$ for later use.

■ PAUSE POINT It is highly recommended to use freshly prepared QD705-RGD conjugate for cell staining or *in vivo* tumor imaging. We found that QD705-RGD can be stored for up to a few weeks without significant aggregation. However, storing it for several months is not recommended.

? TROUBLESHOOTING

Characterization of the RGD peptide-conjugated QDs

10| Determine the concentration of the collected fraction(s) with a fluorometer using serial dilutions of the original QD705 solution as the standard. Typically, a series of concentrations between 0.01 and 10 nM will suffice. Determine the QD705-RGD concentration in triplicate samples using the standard curve. Dilution is necessary, as the collected QD705-RGD fractions are typically between 100 nM to a few μM in concentration.

11| Prepare ^{125}I -echistatin solution in cell-binding buffer (e.g., 0.5 $\mu\text{Ci ml}^{-1}$). Typically about 50 μl of solution will be needed per well.

! CAUTION It is imperative to obtain appropriate training previously and abide by all regulatory rules when handling radioactivity.

12| Prepare three stock solutions of different concentration QD705-RGD conjugate (e.g., 2, 20 and 200 nM) in cell-binding buffer. We recommend that parallel experiments using the unconjugated RGD peptide also be carried out (concentrations of stock solutions: 20, 200 and 2 μM) for direct comparison of the integrin $\alpha_v\beta_3$ -binding affinity between QD705-RGD conjugate and the unconjugated RGD peptide. Triplicate samples are recommended.

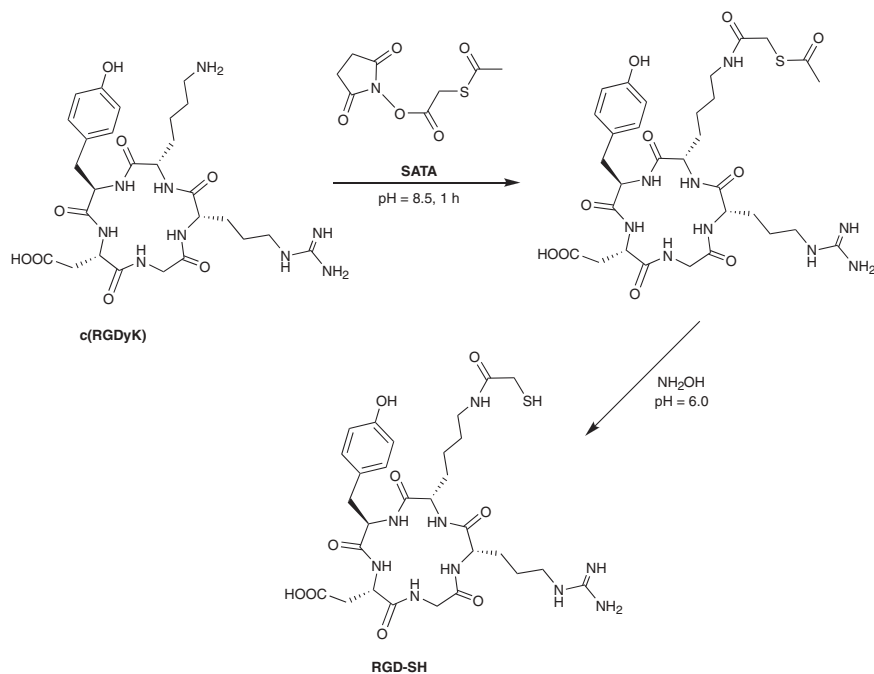


Figure 2 | Converting the amino group in the RGD peptide into a thiol.

13| Add 0.02–0.03 μCi of ^{125}I -echistatin and appropriate volume of the QD705-RGD stock solution to each well in a 96-well plate. Assuming that the final volume is 200 μl per well, the final concentration of the QD705-RGD conjugate should typically range from 10 pM to about 0.1 μM .

? TROUBLESHOOTING

14| From a stock of 2 million U87MG cells ml^{-1} of cell-binding buffer, add 1×10^5 U87MG cells (50 μl) per well, adjust the total volume to 200 μl per well with cell-binding buffer and incubate for 2 h at room temperature.

15| Use the vacuum manifold to remove the incubation buffer from the 96-well plate and wash three times with cell-binding buffer (100 μl per well).

16| Heat-dry the 96-well plate in the dry bath incubator until the filter membrane is dry. This usually takes about 15 min.

17| Collect the membrane from each well into polystyrene culture test tubes.

■ **PAUSE POINT** The radioactivity on each membrane can be measured later, as ^{125}I has a half-life of 60 d.

18| Measure the radioactivity on each membrane with a γ -counter.

19| Fit the data by nonlinear regression and calculate the best-fit IC_{50} (inhibitory concentration of 50%) values for U87MG cells. QD705-RGD should have much lower IC_{50} values (higher binding affinity) than the unconjugated RGD peptide.

20| Assuming that the QD705-RGD conjugate is functional, they can be used for either cell staining (Option A) or *in vivo* tumor imaging (Option B).

(A) Cell staining

(i) Pre-seed 0.1×10^5 U87MG cells (integrin $\alpha_v\beta_3$ -positive) in each glass-bottomed microwell dish and incubate overnight.

Parallel experiments using integrin $\alpha_v\beta_3$ -negative MCF-7 cells should also be carried out as a control.

(ii) Prepare 1 nM solution of QD705 and QD705-RGD in cell-binding buffer (1 ml of each usually suffice).

? TROUBLESHOOTING

(iii) Aspirate the cell culture medium from the dish.

(iv) Wash the cells 2–3 times with 1 ml of cell-binding buffer (3–5 min each).

(v) Add 150–300 μl of the QD705 or QD705-RGD solution to each dish.

(vi) Incubate the dishes in the incubator (37 °C) for about 30 min.

(vii) Aspirate the staining solution, wash with cell-binding buffer for 3 times (3–5 min each).

(viii) Add 500–600 μl cell-binding buffer to each dish and examine the cells under a microscope.

? TROUBLESHOOTING

(B) *In vivo* tumor imaging

(i) Check and make sure that the U87MG tumor size is about 500 mm^3 .

(ii) Set up the Maestro imaging system.

(iii) Set up the IVIS imaging system.

(iv) Anesthetize the animals using the rodent anesthesia system with isoflurane (2% (vol/vol) isoflurane in 0.2 l min^{-1} of O_2 flow).

(v) Inject about 200 pmol of QD705-RGD solution in each mouse via tail vein (total volume, 100–200 μl). We recommend injecting some PBS (about 50 μl) afterward to flush the tail vein.

(vi) Scan the animal with either or both imaging systems at serial time points post-injection. We typically choose 10 min, 1 h, 4 h, 12 h and 24 h. Image acquisition time ranges from a few seconds to a few minutes per scan.

(vii) For the IVIS imaging system, there is minimal image processing, except adjusting the minimum and maximum value of the color scale. For the Maestro imaging system, spectral unmixing (separating the fluorescence signals of different fluorophores based on the emission spectra^{33,34}) is needed, which can be done either with the automatic feature embedded in the software or manually. For manual unmixing, the autofluorescence spectrum should be obtained from a normal mouse without QD injection. QD spectrum can be obtained by subtraction of the autofluorescence signal from the mixed signal of a mouse injected with QD705-RGD (e.g., the liver or the U87MG tumor). The unmixed mouse autofluorescence and QD fluorescence images can be color-coded differently and merged.

(viii) If needed, harvest the tumor and major organs and image them again using the IVIS and the Maestro system.

Ex vivo tissue staining and measuring the tissue homogenate fluorescence can also be carried out to validate the *in vivo* imaging results.

● **TIMING**

Preparation of the peptide-conjugated QDs takes about 3–4 h.

Cell-binding assay usually takes 5–8 h, depending on how many samples are used.

Cell staining typically takes about 2–3 h, excluding pre-seeding the cells the day before and determining the concentration of peptide-conjugated QDs with a fluorometer.

? TROUBLESHOOTING

Step 9

If the peptide-conjugated QD has been stored for a long period, some aggregation may occur and it will severely interfere with the cell staining and *in vivo* imaging. For cell staining, the aggregates are very bright, hard to wash away and will overshadow the fluorescence signal resulted from specific RGD-integrin $\alpha_v\beta_3$ binding. For *in vivo* imaging, the aggregates may be trapped in the lung due to the large size. Typically, centrifuge the peptide-conjugated QD at 8,000 r.p.m. at 4 °C in a microcentrifuge for 10 min and only use the supernatant to avoid such problems.

Step 13

Using multiple-channel pipettes can significantly reduce the time of adding the cells and ^{125}I -echistatin. However, adding serial concentrations of QD705-RGD or RGD solutions to each well is rather time consuming and prone to error. It takes practice to become proficient. All the ^{125}I -containing radioactive waste needs to be collected and disposed under the guidance of the institutional radiation safety office.

Step 20A(ii)

The presence of certain metal ions (e.g., Mn^{2+} and Mg^{2+}) in the cell-binding buffer is essential for integrin $\alpha_v\beta_3$ staining. The cyclic RGD peptide binds at the major interface between the α_v and β_3 subunits and makes extensive contacts with both in a transition metal-dependent mode^{35,36}. Binding buffer without these ions will result in low counts of the collected membrane. Newly purchased ^{125}I -echistatin is recommended for more reliable/accurate results. Using ^{125}I -echistatin after more than two half-lives (~4 months) will also lead to low counts.

Blocking experiments may also be carried out to confirm the integrin $\alpha_v\beta_3$ specificity of the staining. Typically, we use 1 μM RGD peptide for blocking. As the blocking solution may cause detachment of the cells from the dish, it is important that the cells are attached well to the glass slip for such blocking studies. Wash the cells with extra care.

Step 20A(viii)

Such fluorescence-based cell staining is semi-quantitative. It is essential that all the cell-staining experiments are carried out using the same experimental procedure and microscope setup. The fluorescence images acquired with the microscope should be displayed at the same pseudocolor scale. Most fluorescence microscope automatically displays the acquired images in 'autoscale' mode and this can be misleading. The image processing software is usually pre-installed on the computer that comes with the microscope. Alternatively, images can also be acquired with a confocal microscope, which may give additional information regarding to what extent the QD705-RGD is internalized upon integrin $\alpha_v\beta_3$ binding (integrin $\alpha_v\beta_3$ is a membrane-bound receptor and the RGD-binding domain is in the extracellular loop).

ANTICIPATED RESULTS

Results from a typical competitive cell-binding assay of RGD and QD705-RGD using ^{125}I -echistatin as the radioligand are shown in **Figure 3**. Compared with the unconjugated RGD peptide, QD705-RGD should have much stronger integrin $\alpha_v\beta_3$ -binding affinity. Gel electrophoresis has been carried out to confirm the conjugation of proteins on QDs^{27,28}. However, whether attaching multiple copies of small peptides such as RGD will result in a significantly shifted band has not been tested. QD705-RGD has integrin $\alpha_v\beta_3$ -specific staining on integrin $\alpha_v\beta_3$ -positive U87MG cells, whereas QD705 has only minimal nonspecific binding, as shown in **Figure 4**.

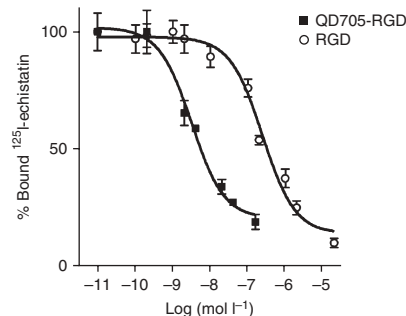


Figure 3 | Inhibition of ^{125}I -echistatin (integrin $\alpha_v\beta_3$ -specific) binding to $\alpha_v\beta_3$ integrin on U87MG cells by RGD peptide and QD705-RGD ($n = 3$, mean \pm SD). The IC_{50} values for the RGD peptide and QD705-RGD are 255 and 3.3 nM, respectively.

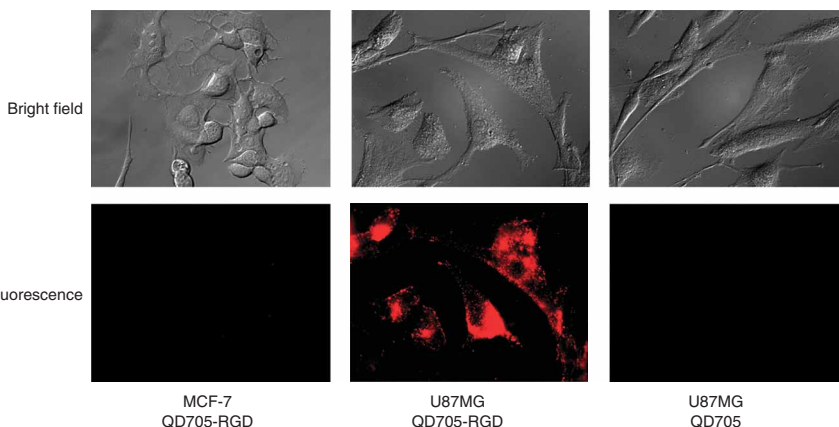


Figure 4 | Staining of live human breast cancer MCF-7 cells (integrin $\alpha_v\beta_3$ -negative) and human glioblastoma U87MG cells (integrin $\alpha_v\beta_3$ -positive) using 1 nM of QD705-RGD. Staining of U87MG cells with 1 nM of QD705 are also shown. Filter set: excitation, 420/40 nm; emission, 705/40 nm. Magnification: $\times 400$. All fluorescence images were acquired under the same conditions and displayed under the same scale.

Representative images of U87MG tumor-bearing mice (injected with 200 pmol of QD705 or QD705-RGD) acquired using the Maestro and the IVIS systems are shown in **Figure 5**. In our study, fluorescence signal resulting from QD705-RGD was clearly visible with both equipments. With the spectral unmixing capability of the Maestro system, it is unambiguous in differentiating the QD705-RGD fluorescence signal from the mouse autofluorescence, which was not possible for the IVIS system used in this study. When using the Maestro system, the typical unmixed emission spectra of QD705-RGD and mouse autofluorescence are shown in **Figure 5b**.

QD705-RGD mainly targets the tumor vasculature integrin $\alpha_v\beta_3$ due to the short circulation half-life²⁰. *Ex vivo* immunofluorescence staining of the tumor vessels confirmed that the vast majority of injected QD705-RGD does not extravasate from the tumor vessels^{20,30}. For other vasculature-related targets, the expression level of the target on the vasculature needs to be sufficiently high to observe good tumor contrast. Based on our experience, the QDs we tested are not suitable for targets that are present only on the tumor cells, as the majority of the QD-based conjugate never escaped the circulation to reach the tumor cells.

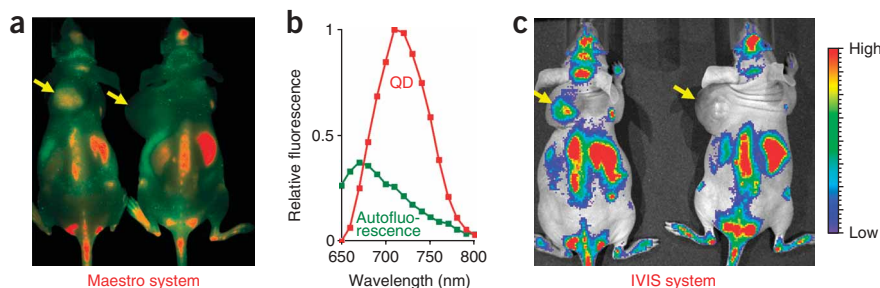


Figure 5 | *In vivo* imaging of U87MG tumor-bearing mice (yellow arrows) at 6 h post-injection of 200 pmol of QD705-RGD (left) or QD705 (right). (a) For the Maestro system, the mice autofluorescence is color-coded green and the unmixed QD signal is color-coded red. (b) The ‘pure’ autofluorescence and QD spectra used for spectral unmixing. (c) Image of the same mouse acquired with the IVIS system immediately after that acquired with the Maestro system shown in a.

ACKNOWLEDGMENTS This work was supported by the National Cancer Institute (NCI) Center of Cancer Nanotechnology Excellence (CCNE) grant U54CA119367 and R21 CA121842.

AUTHOR CONTRIBUTIONS W.C. and X.C. did the conjugation. W.C. did the imaging experiments and analyzed the data. W.C. and X.C. designed and carried out research. W.C. and X.C. wrote the manuscript.

Published online at <http://www.natureprotocols.com>
Reprints and permissions information is available online at <http://npg.nature.com/reprintsandpermissions>

- Cai, W., Hsu, A.R., Li, Z.B. & Chen, X. Are quantum dots ready for *in vivo* imaging in human subjects? *Nanoscale Res. Lett.* **2**, 265–281 (2007).
- Michalet, X. *et al.* Quantum dots for live cells, *in vivo* imaging, and diagnostics. *Science* **307**, 538–544 (2005).
- Medintz, I.L., Uyeda, H.T., Goldman, E.R. & Mattoussi, H. Quantum dot bioconjugates for imaging, labelling and sensing. *Nat. Mater.* **4**, 435–446 (2005).
- Alivisatos, A.P., Gu, W. & Larabell, C. Quantum dots as cellular probes. *Annu. Rev. Biomed. Eng.* **7**, 55–76 (2005).
- Li, Z.B., Cai, W. & Chen, X. Semiconductor quantum dots for *in vivo* imaging. *J. Nanosci. Nanotechnol.* **7**, 2567–2581 (2007).
- Frangioni, J.V. *In vivo* near-infrared fluorescence imaging. *Curr. Opin. Chem. Biol.* **7**, 626–634 (2003).
- Dubertret, B. *et al.* *In vivo* imaging of quantum dots encapsulated in phospholipid micelles. *Science* **298**, 1759–1762 (2002).
- Voura, E.B., Jaiswal, J.K., Mattoussi, H. & Simon, S.M. Tracking metastatic tumor cell extravasation with quantum dot nanocrystals and fluorescence emission-scanning microscopy. *Nat. Med.* **10**, 993–998 (2004).
- Larson, D.R. *et al.* Water-soluble quantum dots for multiphoton fluorescence imaging *in vivo*. *Science* **300**, 1434–1436 (2003).
- Stroh, M. *et al.* Quantum dots spectrally distinguish multiple species within the tumor milieu *in vivo*. *Nat. Med.* **11**, 678–682 (2005).
- Kim, S. *et al.* Near-infrared fluorescent type II quantum dots for sentinel lymph node mapping. *Nat. Biotechnol.* **22**, 93–97 (2004).
- Zimmer, J.P. *et al.* Size series of small indium arsenide-zinc selenide core-shell nanocrystals and their application to *in vivo* imaging. *J. Am. Chem. Soc.* **128**, 2526–2527 (2006).
- Thorne, R.G. & Nicholson, C. *In vivo* diffusion analysis with quantum dots and dextrans predicts the width of brain extracellular space. *Proc. Natl. Acad. Sci. USA* **103**, 5567–5572 (2006).

- Mammen, M., Chio, S. & Whitesides, G.M. Polyvalent interactions in biological systems: implications for design and use of multivalent ligands and inhibitors. *Angew. Chem. Int. Ed. Engl.* **37**, 2755–2794 (1998).
- Cai, W. & Chen, X. Anti-angiogenic cancer therapy based on integrin $\alpha_v\beta_3$ antagonism. *Anti-Cancer Agents Med. Chem.* **6**, 407–428 (2006).
- Cai, W., Rao, J., Gambhir, S.S. & Chen, X. How molecular imaging is speeding up anti-angiogenic drug development. *Mol. Cancer Ther.* **5**, 2624–2633 (2006).
- Bergers, G. & Benjamin, L.E. Tumorigenesis and the angiogenic switch. *Nat. Rev. Cancer* **3**, 401–410 (2003).
- Hood, J.D. & Chersesh, D.A. Role of integrins in cell invasion and migration. *Nat. Rev. Cancer* **2**, 91–100 (2002).
- Hynes, R.O. Integrins: bidirectional, allosteric signaling machines. *Cell* **110**, 673–687 (2002).
- Cai, W. *et al.* Peptide-labeled near-infrared quantum dots for imaging tumor vasculature in living subjects. *Nano Lett.* **6**, 669–676 (2006).
- Hermanson, G.T. *Bioconjugate Techniques* (Academic Press, San Diego, CA, USA, 1996).
- Cai, W. *et al.* *In vitro* and *in vivo* characterization of ⁶⁴Cu-labeled Abegrin, a humanized monoclonal antibody against integrin $\alpha_v\beta_3$. *Cancer Res.* **66**, 9673–9681 (2006).
- Liu, Z. *et al.* *In vivo* biodistribution and highly efficient tumour targeting of carbon nanotubes in mice. *Nat. Nanotechnol.* **2**, 47–52 (2007).
- Cao, Q. *et al.* Combination of integrin siRNA and irradiation for breast cancer therapy. *Biochem. Biophys. Res. Commun.* **351**, 726–732 (2006).
- Pradhan, N., Battaglia, D.M., Liu, Y. & Peng, X. Efficient, stable, small, and water-soluble doped ZnSe nanocrystal emitters as non-cadmium biomedical labels. *Nano Lett.* **7**, 312–317 (2007).
- Pradhan, N. & Peng, X. Efficient and color-tunable Mn-doped ZnSe nanocrystal emitters: control of optical performance via greener synthetic chemistry. *J. Am. Chem. Soc.* **129**, 3339–3347 (2007).
- So, M.K., Xu, C., Loening, A.M., Gambhir, S.S. & Rao, J. Self-illuminating quantum dot conjugates for *in vivo* imaging. *Nat. Biotechnol.* **24**, 339–343 (2006).
- So, M.K., Loening, A.M., Gambhir, S.S. & Rao, J. Creating self-illuminating quantum dot conjugates. *Nat. Protoc.* **1**, 1160–1164 (2006).
- Mulder, W.J. *et al.* Quantum dots with a paramagnetic coating as a bimodal molecular imaging probe. *Nano Lett.* **6**, 1–6 (2006).
- Cai, W., Chen, K., Li, Z.B., Gambhir, S.S. & Chen, X. Dual-function probe for PET and near-infrared fluorescence imaging of tumor vasculature. *J. Nucl. Med.* **48**, 1862–1870 (2007).
- Cai, W. *et al.* Quantitative PET of EGFR expression in xenograft-bearing mice using ⁶⁴Cu-labeled cetuximab, a chimeric anti-EGFR monoclonal antibody. *Eur. J. Nucl. Med. Mol. Imaging.* **34**, 850–858 (2007).



32. Cai, W. *et al.* PET of vascular endothelial growth factor receptor expression. *J. Nucl. Med.* **47**, 2048–2056 (2006).
33. Levenson, R.M. Spectral imaging and pathology: seeing more. *Lab. Med.* **35**, 244–251 (2004).
34. Mansfield, J.R., Gossage, K.W., Hoyt, C.C. & Levenson, R.M. Autofluorescence removal, multiplexing, and automated analysis methods for in-vivo fluorescence imaging. *J. Biomed. Opt.* **10**, 41207 (2005).
35. Xiong, J.P. *et al.* Crystal structure of the extracellular segment of integrin $\alpha_v\beta_3$. *Science* **294**, 339–345 (2001).
36. Xiong, J.P. *et al.* Crystal structure of the extracellular segment of integrin $\alpha_v\beta_3$ in complex with an Arg-Gly-Asp ligand. *Science* **296**, 151–155 (2002).
37. Cai, W., Zhang, X., Wu, Y. & Chen, X. A thiol-reactive ^{18}F -labeling agent, *N*-[2-(4- ^{18}F -fluorobenzamido)ethyl]maleimide (^{18}F -FBEM), and the synthesis of RGD peptide-based tracer for PET imaging of $\alpha_v\beta_3$ integrin expression. *J. Nucl. Med.* **47**, 1172–1180 (2006).
38. Jue, R., Lambert, J.M., Pierce, L.R. & Traut, R.R. Addition of sulfhydryl groups to *Escherichia coli* ribosomes by protein modification with 2-iminothiolane (methyl 4-mercaptobutyrimidate). *Biochemistry* **17**, 5399–5406 (1978).